CrossMark

Investigation of the textural and adsorption properties of activated carbon from HTC and pyrolysis carbonizates

Catalina Rodríguez Correa[1] · Chatri Ngamying[1,2] · Dietmar Klank[3] · Andrea Kruse[1]

Abstract Bamboo was converted into a microporous activated carbon (AC) following either a one- or a two-step activation process with KOH. The main objective was to analyze the influence of the carbonization process (pyrolysis and hydrothermal carbonization (HTC)) and mixing method of KOH (dry mixing or impregnation) on the AC textural properties as well as on the adsorption capacity of water-soluble pollutants and hydrogen (H_2) storage. The highest AC yields were obtained after a two-step activation process. These ACs presented the largest surface areas (2000–2500 m^2 g^{-1}) and the best adsorption capacities not only in aqueous media but also of H_2. The type of carbonization process did not have a significant effect on yield and adsorption capacities, but it did affect the surface area and pore size distribution. HTC led to ACs with a larger total pore volume than ACs from pyrolysis, but the microporous surface area was smaller. KOH impregnation led to slightly but significantly higher yields than mixing KOH dry; yet, the textural and adsorption properties were not significantly improved. KOH impregnation led to slightly but significantly higher yields than mixing KOH dry; yet, the surface area and pore size distribution as well as

adsorption properties were not significantly improved. H_2 adsorption capacity was highest for ACs from impregnated hydrochar, followed closely by ACs from pyrochars.

1 Introduction

Uncontrolled and improper waste management, the reliability of industrial development on fossil resources together with the extensive population growth are significant contributors to climate change. One of the most notorious consequences of climate change is the depletion and contamination of water sources, which in turn threatens aspects like food security, economic development, and life quality [1]. For this reason, water treatment processes as well as the development of adsorbents, such as activated carbon (AC), have become strong research fields. ACs are key materials for removing impurities from polluted water and have shown to be effective in wastewater treatment applications [2, 3]. Additionally, ACs are the most widespread material used in gas storage and separation systems [4, 5]. The AC properties are strongly dependent on the precursor as well as on the activation process. Typical precursors from renewable resources are wood and coconut shell. Bamboo has been studied as possible precursor to produce AC physically as well as chemically, and the results have been promising [6–8]. There is even a feasibility study carried out by Choy et al. [9], where they demonstrate that it can be profitable to chemically produce AC from bamboo and KOH.

Bamboo is a plant native from Asia with excellent physical and mechanical properties (e.g., compression strength, Young's modulus, and bending strength) [10, 11]. Its fast growth, versatility, low weight, and low cost make bamboo a

✉ Catalina Rodríguez Correa
c.rodriguez@uni-hohenheim.de

1 Department of Conversion Technology and LCA of Renewable Resources, University of Hohenheim, Institute of Agricultural Engineering, Garbenstrasse 9, 70599 Stuttgart, Germany

2 Faculty of Agriculture, Chiang Mai University, 239 Huay Keaw Road, Suthep, Muang, Chiang Mai 50200, Thailand

3 Quantachrome GmbH & Co. KG, 85235 Odelzhausen, Germany

⌂ Springer

promising feedstock for the production of goods used on an everyday basis, as well as in the food, textile, and paper industries [12]. Bamboo is not only important for economic purposes but also has a positive impact on the environment; it promotes carbon sequestration, limits soil erosion in cropping systems, supports bioremediation, improves groundwater quality, and increases the organic matter in soils, lowering the demand for artificial fertilizers [13, 14]. This woody plant has a high lignin and cellulose content in addition to a low water content [15, 16], making it a suitable candidate for pyrolysis. Pyrolysis is a thermochemical conversion process that takes place at temperatures higher than 350 °C and oxygen absence. During this process, biomass polymeric chains (cellulose, lignin, and hemicellulose) are irreversibly thermally degraded into solid (pyrochar), tars, and a gaseous mixture of CO, CO_2, H_2O, H_2, and short-chain hydrocarbons [17]. At pyrolysis conditions, biomass decomposition is limited due to slow heat transfer. From a macroscopic perspective, particle size is the most influencing factor regarding heat transfer limitations. When small particles are used, heat transfer occurs more efficiently; thus, the production of liquid and gas products is favored and a small char amount is yielded. Thermogravimetric studies with biomass have shown that each biomass component decomposes at different temperatures and with no interaction between each other. The same experiments with model substances and mixtures of model substances showed the same temperature dependence as biomass, but the decomposition rates were slightly slower. This has been attributed to heat transfer limitations due to char formation from the carbonization of the components that decompose at lower temperatures (e.g., the heat transfer necessary for the decomposition of cellulose is limited by the char formed from hemicellulose) [18, 19]. A recent study conducted by George et al. has shown that isolated lignins and mixtures of lignin and cellulose produced larger char yields than lignins embedded in biomasses. This leads to the conclusion that there might some synergies occurring between the biomass components during pyrolysis as a result of the intricate intermeshing of the natural polymers [20].

Another carbonization process suitable to convert biomass into a carbon-rich product is hydrothermal carbonization (HTC). This technology is an interesting approach not only for carbonizing wet biomass but also for feedstock with a small particle size, like sawdust. Under HTC conditions, the heat transfer occurs much faster since the reaction takes place in water. When covered by water, biomass particles swell, which allows a more homogeneous decomposition. Additionally, the char yield is substantially higher since lignin decomposition is unsubstantial. Another advantage of using HTC compared to pyrolysis is that the decomposition reactions take place at significantly lower temperatures (180–250 °C) in a closed system. During HTC, mostly carbohydrates (cellulose and hemicellulose) are degraded by means of hydrolysis reactions. Lignins are mostly left unreacted, since only some chemical bonds can

be hydrolyzed and most of the chemical structure needs higher temperature to degrade [21]. Dinjus et al. [22] not only observed that lignin decomposes unsubstantially but they also suggested that lignin acts as a protective case that restricts the release of the decomposition products of carbohydrates. The main products are a solid (hydrochar) with higher H/C and O/C ratios compared to pyrochar, water-soluble organic compounds and a gas product, which consists mainly of CO_2.

Carbonized biomass is a suitable precursor to produce AC with similar characteristics than AC from fossil sources. Chemical activation with KOH is a reliable process to obtain highly microporous materials, and the most widespread way to make the mixture of KOH and precursor is through impregnation of a concentrated KOH solution followed by a drying step. After conducting a thorough literature review, few studies focusing on the method for mixing KOH with the precursor were found. One of the first authors that compared impregnation of KOH versus physical (dry) mixing were Ahmadpour and Do [23] using bituminous coal as precursor. They determined that by impregnating the coal with KOH, an AC with a higher surface area as well as micropore volumes was obtained. Also, the mass loss was lower than when they mixed KOH dry. The same authors repeated these experiments using macadamia nutshell as precursor. In terms of textural properties, they arrived to similar results. However, the mass loss was considerably higher (80% for the macadamia versus 25–30% for the coals), independently of the mixing method [24]. Lillo-Ródenas et al. [25, 26] activated Spanish anthracite with NaOH as well as with KOH and arrived to the conclusion that impregnation leads to higher yields, microporosities, and apparent surface areas.

To the authors' knowledge, there are no studies that compare pyrolysis and hydrothermal carbonization as carbonization steps during a two-step activation. For this reason, the main objective of this work was to analyze the influence of the carbonization step and of the KOH mixing process on the textural properties and adsorption potential of chemically ACs using bamboo as precursor and KOH as activating agent. This study shall also contribute to the groundwork for the development of new functional materials from biomass.

2 Materials and methods

2.1 Experimental design

The effects of the carbonization process (no carbonization, hydrothermal carbonization, and pyrolysis) as well as KOH mixing process with the precursor (dry or impregnation) were studied. The experiments followed a completely randomized, 3×2 factorial incomplete block design to keep track of the stability of the different reactors and furnaces over time. Each treatment was repeated twice except for the experiments

involving raw bamboo, which were repeated at least four times due to the low AC yields.

2.2 Feedstock

The selected feedstock was giant bamboo (*Dendrocalamus sericeus*) residues (dry) obtained from Chiang Mai, Thailand. The particle size was reduced based on each carbonization technique: for pyrolysis, bamboo was cut to pieces of approximately $1 \times 0.5 \times 2$ cm; for hydrothermal carbonization (HTC), bamboo was milled to a particle size smaller than 0.5 mm with a Retsch SM 200 cutting mill. A smaller particle size was necessary for HTC to a larger surface area could be in direct contact with water. Only then, the process can be considered a hydrothermal conversion, i.e., a conversion in water. Ultimate and proximate analyses are presented in Table 1.

2.3 Carbonization

2.3.1 Pyrolysis

Pyrolysis was conducted in a quartz glass tube reactor heated externally with a split tube furnace ROK 50/250/11 (ThermConcept Dr. Fischer GmbH & Co. KG; Fig. 1). The reactor was loaded with 200 g of bamboo chips and heated up to 600 °C with a constant heating rate of 10 °C min^{-1}. When the final temperature was achieved, the reaction was held for 2 h. Nitrogen was constantly introduced in the reactor with a flow of 3 1 min^{-1} during the whole process to keep an inert atmosphere. The high flow rates constrained air diffusion towards the inside of the reactor. The pyrochar yield, $Y_{pyrochar}$ (%), was calculated with Eq. 1, where $m_{pyrochar}$ (g) was the pyrochar mass obtained after pyrolysis and m_{bamboo} (g) was the input mass of bamboo as received. After pyrolysis, the product was cooled down to room temperature and it was milled with a Pulverisette 6 classic line ball mill (Fritsch GmbH) to a particle

size smaller than 300 μm. After pyrolysis, the solids were collected for further activation and characterization.

$$Y_{pyrochar}(\%) = \frac{m_{pyrochar}}{m_{bamboo}} \times 100 \tag{1}$$

2.3.2 Hydrothermal carbonization

Hydrothermal carbonization (HTC) was conducted in 250-ml stainless steel (1.4401) high pressure autoclaves filled to 75% of its maximum capacity with a mixture of 20 wt% dry bamboo and 80 wt% deionized water. The mixture was prepared by stirring the ground biomass with water until the biomass was fully covered by water. The autoclaves were heated up to 250 °C in the furnace of a gas chromatograph Series II 5890 (Hewlett-Packard). The reaction time lasted 3 h, and temperature as well as pressure were monitored with a data logger RSG 30 (Endress+Hauser AG). After the reaction time was completed, the autoclaves were quenched with water until a temperature lower than 50 °C inside the autoclave was reached. The liquid and solid fractions were filtered, and the hydrochar was washed with distilled water until the electrical conductivity of the filtrate was lower than 15 μS cm^{-1}. The hydrochars were dried at 105 °C for at least 16 h and were kept for further activation and characterization. The hydrochar yield, $Y_{hydrochar}$ (%), was calculated with Eq. 2, where $m_{hydrochar}$ (g) was the hydrochar mass obtained after drying and m_{bamboo} (g) was the input mass of bamboo as received.

$$Y_{hydrochar}(\%) = \frac{m_{hydrochar}}{m_{bamboo}} \times 100 \tag{2}$$

2.4 Activation

Chemical activation with KOH was conducted to increase the surface area and microporosity using uncarbonized bamboo or

Table 1 Ultimate and proximate analysis of the feedstock, chars, and activated carbons (AC)

Sample	C_{DAF} (wt%)	H_{DAF} (wt%)	N_{DAF} (wt%)	S_{DAF} (wt%)	$O_{DAF.dif}$ (wt%)	Ash (wt%)	VM_{db} (wt%)	$C_{fix,db}$ (wt%)
Feedstock	46.7	5.8	0.9	N.D.	46.5	2.3	76.6	21.1
Hydrochar	66.8	4.1	1.4	N.D.	27.7	2.0	46.3	51.7
Pyrochar	88.1	1.7	1.6	0.1	8.6	8.0	8.9	83.1
AC raw bamboo—dry	80.7	1.0	0.5	0.05	17.8	3.8	N.M.	N.M.
AC raw bamboo—impregnated	77.3	1.0	0.9	0.02	20.8	4.5	N.M.	N.M.
AC hydrochar—dry	83.2	0.8	0.5	0.01	15.5	1.4	N.M.	N.M.
AC hydrochar—impregnated	84.7	1.5	1.1	0.13	12.7	7.3	N.M.	N.M.
AC pyrochar—dry	83.3	0.9	0.4	N.D.	15.4	4.8	N.M.	N.M.
AC pyrochar—impregnated	77.2	1.1	0.5	N.D.	21.2	5.4	N.M.	N.M.

The chemical composition is given on a dry and ash free basis (DAF). The oxygen was calculated by difference (dif). Volatile matter (VM) and fixed carbon (C_{fix}) were calculated on a dry basis (db)

N.D. not detected, *N.M.* not measured

Fig. 1 Schema of the pyrolysis experimental setup
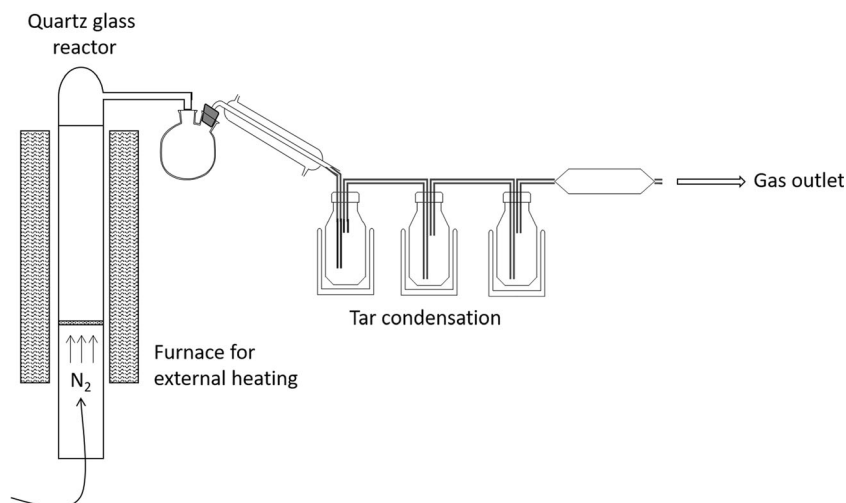
the chars as precursors. The precursor-to-KOH mass ratio was 1:4, and KOH was mixed either as a solid powder (dry activation) or mixed with four parts of distilled water to form a paste together with the char (impregnation). The impregnated mixtures were dried at 105 °C for at least 24 h. All mixtures were prepared in nickel crucibles, which were heated inside a stainless steel batch reactor. The reactor was heated up inside a muffle furnace (Nabertherm GmbH) that had been previously heated up to 600 °C (reaction temperature). This reaction temperature was chosen based on the thermal stability of the pyrolysis char. Since the char was produced at 600 °C, it remained thermally stable at this temperature and, therefore, the effects measured corresponded only to activation. At higher temperatures, the char not only undergoes an activation but also to a further decomposition. The reactor reached 600 °C in approximately 70 min, after which the samples were left to react for 2 h under a constant N_2 flow of 5 l min^{-1}. The temperature inside the reactor was monitored with thermocouples connected to a data logger RSG 30 (Endress+Hauser AG). When the reaction time was completed, the reactor was removed from the furnace and was let to cool down to room temperature under constant N_2 flow (20 l min^{-1}). Afterwards, the solid product was removed from the crucibles by adding HCl (2 M) and filtering it with hot distilled water until the filtrate had an electrical conductivity lower than 15 μS cm^{-1}. The AC was dried for at least 16 h and stored for further characterization.

2.5 Characterization

2.5.1 Chemical composition analysis

C, H, N, and S contents were measured at 1000 °C in a Euro EA CHNSO Elemental Analyzer (HEKAtech) according to the DIN standard 51732 [27]. Ash contents were determined at 550, 815, and 650 °C for bamboo, chars, and ACs, respectively, following the corresponding DIN standards 14775

[28], 51719 [29], and 12902 [30]. The AC quantity obtained from uncarbonized bamboo was not enough to analyze the ash content as per the DIN standard; therefore, it was determined by means of thermogravimetric analysis following the ASTM standard D7582-12 [31]. Volatile matter and fixed carbon (C_{fix}) contents were determined as per the DIN standards 51720 [32] and 51734 [33], respectively.

2.5.2 Textural characterization

Apparent BET surface areas (S_{BET}) as well as total micropore volumes and areas were determined for the textural characterization. S_{BET}s were calculated from N_2 isotherms at 77 K and CO_2 isotherms at 273 K using the Brunauer, Emmett, and Teller model and following the standard ISO 9277:2010 [34]. The N_2 and CO_2 isotherms were measured in an Quadrasorb SI and a Nova from Quantachrome Instruments, respectively, after the samples were degasified at 250 °C for at least 16 h. To control the decomposition degree of the sample at this temperature, TGA analyses of the activated carbons were conducted for at least 16 h (s. "Supplementary materials"). The total micropore volumes and areas were calculated applying the t-plot model to the relative pressure range 0.2–0.5 of the N_2 isotherms. The pore size distribution as well as the average pore size were calculated from the CO_2 isotherms using the density functional theory (DFT) [35].

2.5.3 Adsorption capacity in aqueous media

The adsorption capacity of the ACs was studied by measuring the maximum adsorbed amount of methylene blue, phenols, and iodine in aqueous solution. For this, 0.1 g of AC previously dried at 105 °C were mixed with 100 ml of methylene blue or phenol solutions with concentrations of 750 and 1000 mg l^{-1}, respectively. The mixtures were constantly stirred at room temperature during 24 h to ensure that equilibrium was reached. Subsequently, the samples were filtered

using a Whatman filter paper (40 μm) previously saturated with the solution to determine the final concentration of the liquid fraction. For this, a DR600 spectrophotometer (Hach-Lange) was set at a wavelength of 664 nm for methylene blue and a cuvette fast test LCK 346 (5–200 mg l^{-1}) from Hach-Lange was used for phenols. The equilibrium concentration q_e (mg g^{-1}) was calculated with Eq. 3, where C_0 (mg l^{-1}) is the initial solution concentration, C_e (mg l^{-1}) is the solution concentration at equilibrium, V (l) is the solution volume, and W (g) is the AC mass after drying.

$$q_e = \frac{(C_o - C_e) \times V}{W} \tag{3}$$

Iodine number was estimated with a single-point isotherm following the AWWA B600-78 standard and using a TitroLine 7000 automatic titrator (SI Analytics).

2.6 Adsorption capacity for hydrogen storage

Hydrogen (H$_2$) adsorption isotherms were measured for the ACs that presented the largest surface areas. The isotherms were measured at 77 K in an Autosorb IQ (Quantachrome Instruments) for a pressure range between and 8×10^{-6} and 1 bar. Prior to the measurement, the samples were degasified at 250 °C for at least 16 h.

2.7 Statistical analysis

An analysis of variance was done with the statistical software SAS to estimate the means and standard errors of the yield, methylene blue adsorption capacity, iodine number, phenol adsorption capacity, and BET surface areas. For this, a two-factorial linear model with all factors fixed was used (Eq. 4).

$$y = block + carbonization + activation \\ + carbonization \times activation \tag{4}$$

The presence or absence of interactions between factors was evaluated using an f-test, and the significant differences between the means were determined with a t test. In all cases, the significance level was set at 0.05. Variance homogeneity and normal distribution were visually inspected from the residual plots.

3 Results and discussion

3.1 Carbonization

Pyrolysis and HTC were used as carbonization steps prior to the activation. During both processes, lignocellulosic material underwent a decomposition; yet, the reaction mechanisms were different in each case. For this reason, solid products with different properties were obtained. This was observed from the ultimate and proximate analysis presented in Table 1. Compared to the feedstock, the products from both carbonization processes had higher carbon contents and lower oxygen, nitrogen, and hydrogen contents. However, the HTC product (hydrochar) had a significantly higher oxygen content than the pyrolysis product (pyrochar). Bamboo is composed of approximately 45% cellulose, 22% hemicellulose, and 25% lignin [15, 16]. Based on thermogravimetric experiments, under pyrolytic conditions and at 600 °C cellulose and hemicellulose decompose completely, lignin undergoes a partial but strong decomposition [36]. This thermochemical conversion occurs mainly through fragmentation, decarboxylation, decarbonylation, and dehydration reactions that lead to a strong oxygen and hydrogen loss in the form of H$_2$O, CO$_2$, CO, as well as some H$_2$ and CH$_4$ [37]. Concerning HTC at 250 °C, carbohydrates are the most degraded biomass components due to dehydration and decarboxylation reactions. Consequently, the polymerization of the products from the carbohydrate decomposition takes place. Under HTC conditions, the decomposition of lignin is very low [22]. For this reason, the oxygen loss as well as the production of mainly CO$_2$ are considerably lower compared to pyrolysis [38]. Accordingly, hydrochar is a mixture of the nearly unchanged lignin and the products obtained after the polymerization reactions subsequent to the carbohydrate decomposition [39]. Consequently, the volatile matter of the hydrochars is considerably higher than that of the pyrochars and, in turn, pyrochars have a higher C_{fix} content. Regarding the ash content of hydrochars, it presented a slight decrease compared to bamboo since minerals dissolve in water under hydrothermal conditions [40]. In the case of pyrolysis, most minerals remain within the solid material during the carbonization process and its content increases in the pyrochar due to organic matter losses. Due to the strong oxygen loss during pyrolysis, the pyrochar yield ($Y_{pyrochar} = 26.2 \pm 0.3\%$) was significantly lower (p value <0.001) than the hydrochar yield ($Y_{hydrochar} = 52.9 \pm 0.2\%$).

3.2 Activation

AC yield was calculated based on the initial amount of char as well as on the initial amount of bamboo (Fig. 2). In general, the yields based on the initial amount of char are higher when chars were used as precursors instead of raw biomass. Pyrochar led to the highest amount of AC, followed by hydrochar, and both were significantly higher (p value <0.001) than raw bamboo. The low yields obtained after the activation of raw bamboo agree with several studies; Chandra et al. [41] impregnated raw durian shells with KOH at different ratios and temperatures, which led to yields between 20 and 25% at 650 °C. Muniandy et al. [42] conducted a one-step activation with rice straw using different impregnation ratios, temperatures as well as time, and they reached yields between 16.5 and 18%. To explain this, it is necessary to consider the

Fig. 2 Activated carbon yields obtained after each treatment based on the activation precursor (**a**) and on the initial amount of bamboo (**b**). The *error bars* correspond to the standard error, and the *letters* indicate the significant differences estimated with the statistical model
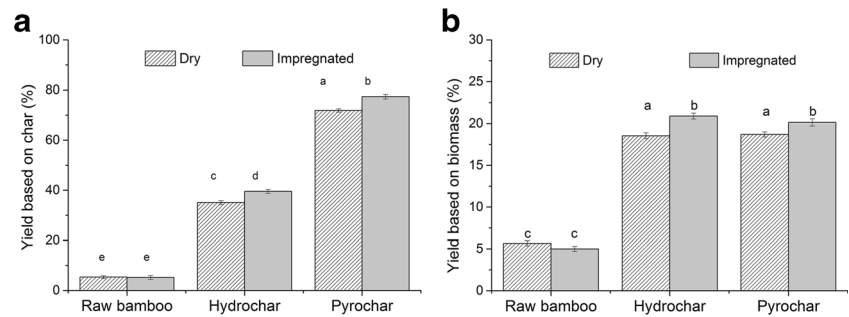
thermal instability of bamboo compared to the chars. During activation, bamboo underwent not only an expansion of its surface area but also a carbonization and a decomposition. It has been demonstrated before that potassium lowers the activation energy of biomass [43] and cellulose [44] during pyrolysis in view of accelerating the feedstock splitting. In other words, it increases especially the gas formation as parallel reaction of the char formation. The effects of potassium have been studied not only by adding potassium but also by removing it through leaching the mineral content of biomass. In both cases, it has been observed that potassium changes the product distribution of pyrolysis by enhancing permanent gases and reducing the tars [45, 46].

Concerning the activation of chars, chemical activation with KOH can be understood as an alkali catalyzed gasification of the biomass [47, 48]. Hydrochar led to higher AC yields (based on char) than raw bamboo, but the yields are lower than when using pyrochar. This can be explained by its lower thermal stability compared to pyrochar. This can be evaluated in terms of the C_{fix} content, which is lower for the hydrochar than for the pyrochar. The AC yields from bamboo hydrochar are comparable to those obtained by Sevilla et al. [49] after activating eucalyptus saw dust with KOH at 700 °C (36 g activated carbons/100 g hydrochar). Hydrochar consists mainly of undecomposed lignin and a carbon-rich product formed after the decomposition of carbohydrates (cellulose and hemicellulose); therefore, it can be expected that the thermal decomposition of hydrochar resembles that of a thermally stable lignin. For this reason, a decomposition/carbonization process takes place at the activation temperature together with an alkali-catalyzed gasification. Regarding the behavior of pyrochar during activation, it can be assumed that pyrochar underwent mostly carbon oxidation (gasification) rather than decomposition (pyrolytic) reactions due to its thermal stability. Pyrochars are thermally stable until the temperature they experienced during their production [50, 51]. The pyrochar used in the current study was produced at 600 °C, which means that it was stable up to this temperature; this indicates that the mass loss experienced during activation was a result of oxidation reactions catalyzed by potassium. If higher activation temperatures were used, not only gasification reactions would occur faster but also parallel decomposition reactions

would take place, analogous to the behavior of hydrochar. From the yields calculated from the initial amount of biomass, it is interesting to observe that there were no significant differences (p value = 0.72 for dry mixing and p value = 0.19 for 1impregnation) between the ACs produced with hydrochar and pyrochar. Based on this, it can be an indication that AC is a state of lower Gibbs free enthalpy and that the path to obtain activated carbon is irrelevant. However, if the yields of the activated carbons from raw bamboo are brought into the discussion, then it is possible to observe that the previous statement is not necessarily true. To understand this, it is necessary to find a common ground between pyrolysis and HTC and that is the decomposition of carbohydrates. In both carbonization processes, carbohydrates decompose fully giving a certain thermal stability and polyaromatic structure to the char. Therefore, to obtain a large surface area and a high activated carbon yield, it might be enough to carbonize the carbohydrates. This makes sense, since lignin already possess a high aromaticity degree as well as a relatively high thermal stability.

Regarding the method employed for mixing the KOH, it was interesting to observe that the yield was significantly higher, if the KOH was mixed by impregnation than as a solid powder (p value = 0.001 for hydrochar and p value = 0.0003 for pyrochars). This agrees with the findings of Ahmadpour and Do [23] and of Lillo-Ródenas et al. [25]. Both groups activated coals from fossil sources with alkali metal hydroxides and obtained lower yields after dry mixing the activating agent than when impregnating the coal with a concentrate solution. A possible explanation are the high temperatures that occurred during the impregnation process. The reaction between KOH and water is extremely exothermic, and it could enhance the reaction between the minerals in the ashes and the potassium hydroxide, leaving less potassium available to react with the carbon [52].

3.2.1 Textural characterization

The textural characterization of ACs comprises the apparent surface area calculated from the Brunauer-Emmett-Teller model (S_{BET}), micropore area (S_{micro}), and volume (V_{micro}) calculated from the t-plot, and the total pore volume ($V_{0.99}$), which is the total volume adsorbed at a relative pressure of 0.99 (Table 2).

These results show that ACs from raw bamboo developed the lowest S_{BET}, V_{micro}, and $V_{0.99}$ compared to the ACs obtained from chars. This can be explained due to pore blockage and pore expansion provoked by decomposition and gasification reactions during the activation process. Hirunpraditkoon et al. [53] activated bamboo impregnated with KOH at 800 °C for different times, and they obtained similar S_{BET} (1169–1533 m² g⁻¹) and $V_{0.99}$ (0.41–0.49) as the AC from raw bamboo presented in the current work. The differences between a one-step (activation of the raw biomass) and a two-step (carbonization followed by an activation) activation were also studied by Basta et al. [54] using rice straw as precursor and impregnation as mixing technique. They arrived to similar results as those presented here: the ACs obtained from a one-step activation led to the lowest yields as well as to the lowest surface areas and porosities. However, the values of the textural properties for rice straw were considerably lower than the ones measured in this study for bamboo. This can be explained by the extremely ash content of rice in addition to its low lignin content [19].

Regarding the ACs obtained from the different chars, there was no significant difference in terms of S_{BET}. However, in terms of pore volume, ACs from pyrochars had a higher micropore volume as well as total pore volume compared to the ACs from hydrochars. Regarding $V_{0.99}$, hydrochars were superior than pyrochars. This can also be observed from the N_2 isotherms presented in Fig. 3a. These isotherms can be classified as type I isotherms and the inflection point, i.e., the point when the activated carbon becomes saturated with gas and the plot becomes a plateau, from the ACs from hydrochar and from pyrochar occur approximately at the same relative pressure and adsorbed volume. This indicates that the internal surface area corresponding to micropores is very similar for both cases (1860–2196 m² g⁻¹ for ACs from hydrochar and 1886–1908 m² g⁻¹ for ACs from pyrochars). However, from the ratio of micropore-to-total surface area can be determined that ACs from pyrochars are composed mainly by micropores (92% of the surface area is microporous), contrary to the others. The isotherms also showed that ACs produced after dry mixing KOH adsorbed more N_2 than those obtained by

impregnation. This is also reflected on the total pore volume, and this difference is particularly marked in the case of ACs from raw bamboo. However, it is relatively small in the case of the ACs obtained from chars.

Figure 3c describes the pore size distribution calculated from the CO_2 isotherms using the DFT theory. Most pores are smaller than 1 nm for all ACs, and ACs from hydrochars have a larger pore volume in this range than those from pyrochar. AC from raw bamboo have the lowest pore distribution.

Contrary to the results presented here, the findings of Lillo-Ródenas et al. [55] showed that pyrolyzing biomass prior to an activation process with alkali metals leads to lower surface areas and pore volumes compared to the activation of raw biomass. A possible explanation for this contradiction are the different process temperatures employed by Lillo-Ródenas et al. [55]. They pyrolyzed the biomass at 850 °C, making the char thermally stable up to this temperature. By activating at 750 °C, the char decomposition was very slow and, therefore, the surface area and porosity development was hindered.

Choy et al. [9] carried out a feasibility study for a plant to produce AC from bamboo and KOH. The calculated economic indices were promising, especially if the production plant was coupled with another facility (e.g., a thermoelectrical plant, a cement manufacturer, or a hazardous waste treatment facility). Given the facts that there are no significant differences between the AC yields obtained from bamboo hydrochars and pyrochars, that there are slight differences between the textural properties of the ACs, and that HTC works at lower temperatures, better economic indices can be expected, if HTC is considered as carbonization step.

3.2.2 Adsorption capacity in aqueous media

The ACs produced from bamboo were tested for their iodine number, methylene blue, and phenol indexes (Fig. 4). AC produced by dry mixing KOH and pyrochar presented the highest adsorption capacity in aqueous media overall. It was closely followed by the AC from impregnated hydrochar. The ACs from impregnated pyrochar and dry mixed hydrochar

Table 2 Textural characterization of all activated carbons

Sample	$S_{BET, N2}$ (m² g⁻¹)	$S_{BET, CO2}$[a] (m² g⁻¹)	V_{micro} (cm³ g⁻¹)	$V_{0.99}$ (cm³ g⁻¹)	$d_{DFT, CO2}$ (nm)	Ratio S_{micro}/S_{BET}
Raw bamboo—dry KOH	1240c ± 225	1082	0.49	0.78	0.82	89%
Raw bamboo—impregnated KOH	1366bc ± 318	923	0.50	0.69	0.82	84%
Hydrochar—dry KOH	2117ab ± 142	1393	0.49	1.14	0.86	85%
Hydrochar—impregnated KOH	2262a ± 183	1990	0.50	1.30	0.57	88%
Pyrochar—dry KOH	1977ab ± 142	1548	0.78	0.97	0.52	92%
Pyrochar—impregnated KOH	2078ab ± 225	1435	0.84	0.95	0.57	92%

The S_{BET} errors and the lower case letters indicating the significant differences were estimated with the statistical model

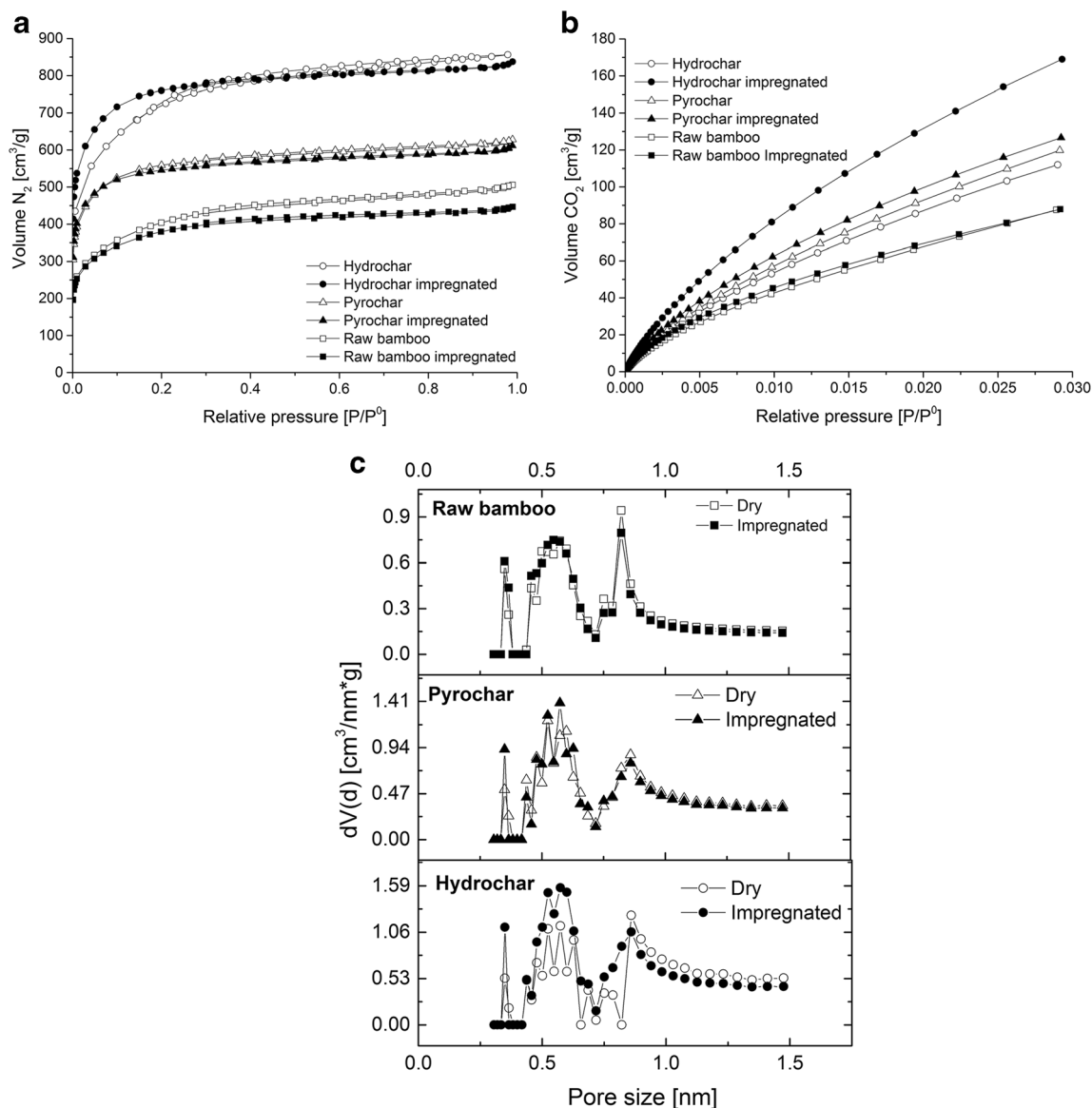[a] Only one sample of the three replicates was measured

Fig. 3 (**a**) N$_2$ isotherms measured at 77 K, (**b**) CO$_2$ isotherms measured at 298 K, and (**c**) pore size distribution calculated from the CO$_2$ isotherm using the DFT model for all activated carbons. The *white and black* *symbols* correspond to the activated carbons produced by dry mixing and impregnation of KOH, respectively

came in third, showing no significant differences between them in any case. The poorest performance was shown by the ACs from raw bamboo, which agrees with the expectations due to its low surface area and pore volumes.

Iodine adsorption, also known as iodine number, is an indicator of the internal surface of a porous solid [56]. In this case, the results show that there are slight, although significant, differences between the ACs and the chars. Nonetheless, the adsorption capacity of these ACs is significantly higher than that from the AC produced from raw bamboo. These results agree with the results shown in Table 2.

Methylene blue and phenol indexes are important parameters that give information regarding adsorption capacity of large molecules and phenolic compounds. Methylene blue

and phenol have a molecular diameter of 1.6 [57] and 0.6 nm [58], respectively. For this reason, it was expected that phenol entered micropores more easily than methylene blue. This was observed in the case of the ACs prepared from the different chars, which adsorbed a larger concentration of phenol molecules (between 3.0 and 3.6 mmol g^{-1}) than of methylene blue (2.2–2.3 mmol g^{-1}). Overall, ACs from pyrochar adsorbed more phenol than those obtained from hydrochar, which is consistent with the fact that the internal surface area of these carbons is composed mainly by micropores. Compared to activated carbons from bamboo studied by different research groups, the adsorption capacity of the ACs described in the current work is remarkably higher and the main explanation is its large microporosity. Wu et al. [59] produced activated
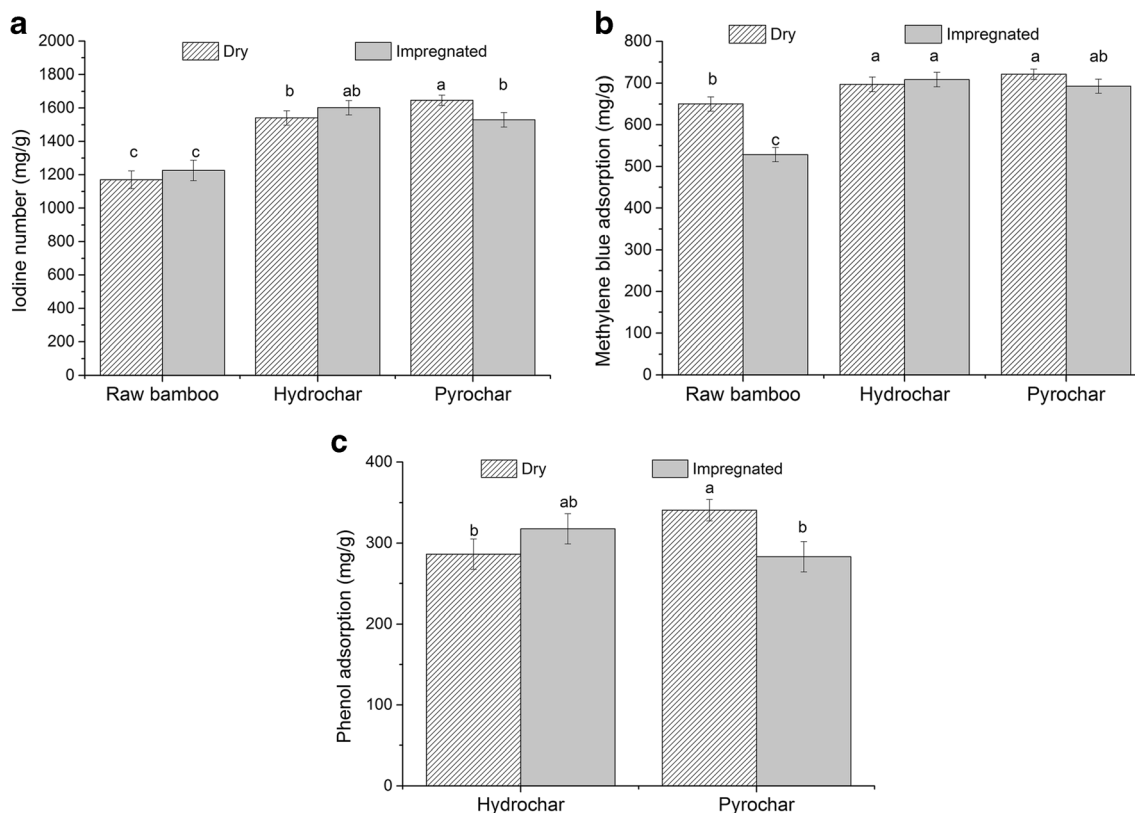
Fig. 4 Iodine number (**a**), methylene blue (**b**), and phenol indexes (**c**). The *error bars* correspond to the standard error, and the *letters* indicate the significant differences estimated with the statistical model

carbon from Makino bamboo following a physical activation process with water steam and by varying reaction temperature and time. The activated carbon produced at the optimal parameters (850 °C for 2 h) developed the best properties including surface area (915 m^2 g^{-1}), average pore size (2.63 nm), and presented the highest iodine number (1044 g kg^{-1}) as well as phenol (approx. 2.2 mol kg^{-1}) and methylene blue (361 g kg^{-1}). Kim et al. [60] used mesoporous activated carbon from bamboo with a surface area of 1329 m^2 g^{-1} to adsorb different dyes and phenol, and they measured a maximum adsorption capacity of approximately 50 mg g^{-1}.

Even though statistics suggest that AC from pyrochar performed the best, the differences between adsorption capacities of the ACs are not large enough to conclude which char or which mixing process produce the AC with the best adsorption capacities in aqueous media.

3.3 Analysis of the activated carbon potentials for hydrogen storage

Physisorption in ACs for hydrogen (H_2) storage is one of the most widespread techniques. This process consists of the weak adsorption of molecules on the carbon surface, and it does not involve changing the molecular nature of H_2 as it happens when storing H_2 in ammonia, formic acid, or in complex metal

hydrides [61]. Due to their large surface areas and high micropore volumes, ACs produced from bamboo pyrochar and hydrochar were analyzed for H_2 adsorption. The maximum H_2 adsorption at 77 K and 1 bar presented by the ACs obtained from hydrochars mixed with dry KOH and impregnated as well as from pyrochars mixed with dry KOH and impregnated were 2.0, 3.2, 2.5, and 2.3 wt%, respectively (Fig. 5). As expected, the AC with the largest surface area and pore volume, namely the AC from bamboo hydrochar impregnated with KOH, showed the largest adsorption capacity. It was followed by both ACs obtained from pyrolysis chars and by the AC from hydrochar mixed with dry KOH. A possible reason to explain the larger adsorption capacities from the AC from impregnated hydrochar is the total pore volume as well as the pore size distribution, since H_2 molecules can enter pores larger than 0.55 nm [62]. As it can be seen from Fig. 3c and Table 2, AC from impregnated hydrochar possessed a slightly higher micropore and total pore volumes than AC from hydrochar mixed with dry KOH. Additionally, AC from impregnated hydrochar had a larger volume of pores with a size close to 0.55 nm. Another influencing factor is the presence of larger micropores, which aid transportation phenomena. AC from hydrochar mixed with dry KOH had a larger average pore size (0.86 nm) than AC from impregnated hydrochar (0.57 nm); however, the volume of pores with a size between 0.6 and 0.8 nm was almost nonexistent in the AC from
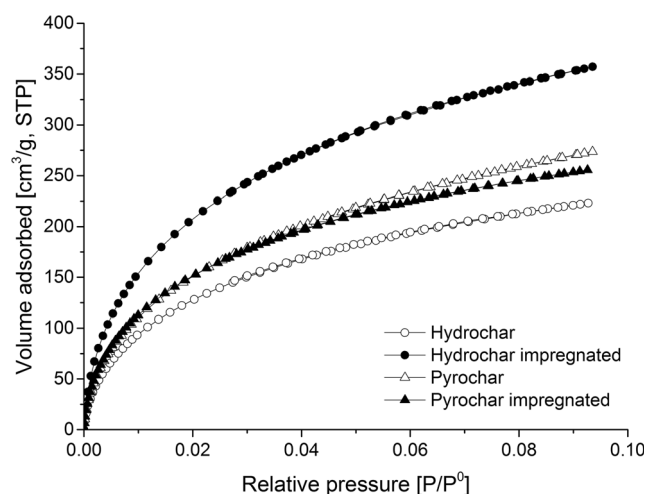
Fig. 5 H_2 isotherms measured at 77 K for the activated carbons with the best textural properties. The *white and black symbols* correspond to the activated carbons produced by dry mixing and impregnation of KOH, respectively

hydrochar mixed with dry KOH. AC from impregnated hydrochar had a larger volume of larger pores, which promoted H_2 diffusion towards the smaller pores. The differences between ACs from pyrochars and AC from impregnated hydrochar can be explained in a similar way. ACs from pyrochars presented a considerably larger micropore volume than AC from hydrochars, but the volume of pores with a size close to 0.55 nm was smaller than that of the AC from impregnated hydrochar. The presence of oxygenated groups can also interfere with the adsorption of hydrogen due to steric hindrance effects and to weaker interactions between hydrogen—oxygen compared to the interactions between hydrogen—and carbon [62]. This could also explain the larger hydrogen adsorption volumes of the AC from impregnated hydrochar, since it has the lowest oxygen content.

Based on the thorough review presented by Thomas [63], the largest adsorbed amount of H_2 at 77 K and 1 bar reported for different carbon materials was approximately 3 wt%. Additionally, those carbon materials with similar BET surface areas to the ACs presented in the present work adsorbed generally H_2 amounts lower than 2.5%. This indicates that the ACs obtained in this study have a superior adsorption capacity than other ACs from nonrenewable precursors with comparable surface areas. Also, the H_2 adsorption was larger than that of most metal oxide frameworks (MOFs) presented in the same review.

Sevilla et al. [49] produced ACs from hydrochars from different organic precursors with slightly lower surface areas and microporosities than those of the ACs presented in this work. Also, the H_2 adsorption capacities at 1 bar were similar. Based on this information and on the fact that there is a rather linear relation between BET surface area and H_2 adsorption capacity [64], it is safe to assume that at higher pressures, the ACs produced from bamboo will adsorb the same amount or slightly more H_2 than those produced by Sevilla et al. [49].

Figure 5 describes the H_2 adsorption isotherms of the ACs. The H_2 isotherms follow a similar trend than the CO_2 and N_2 isotherms. The isotherms showed no hysteresis, implying that the physisorption process is completely reversible at the measurement conditions. This provides some information on the reversible storage capacity (RSC) of the material, which is a determining design parameter [65]. However, experiments involving cycles of H_2 charge and discharge are needed to obtain a better assessment of the RSC of these ACs.

One disadvantage of employing powder AC for H_2 storage is its low bulk density. This could be improved by compressing the powders into pellets or larger particles after. Nonetheless, since pelletizing and binder addition can have a negative effect on the textural properties [66], the losses concerning surface area and pore volumes should be analyzed to evaluate the hydrogen storage potential of pellets.

4 Conclusions

ACs from bamboo were produced following either a one-step or a two-step chemical activation process with KOH as activating agent. KOH was mixed with the precursor either by impregnation or by dry mixing. It was established that a carbonization process is necessary to develop large surface areas and microporosities. On the other hand, the type of carbonization process had no significant effect on yield, but it did affect the textural properties.

ACs produced chemically with KOH from bamboo hydrochar and pyrochar showed promising results to be employed in different applications that involve physisorption processes. The carbonization process had no significant effect regarding adsorption in aqueous media; however, there were clear differences in terms of gas adsorption processes. In this case, ACs from hydrochar adsorbed the highest amount of N_2, CO_2, and H_2.

Despite showing significant differences in terms of yield and adsorption behavior in aqueous media, the mixing method of KOH with the precursor can be considered irrelevant.

References

1. World Health Organization, UNICEF (2015) Progress on sanitation and drinking water: 2015 update and MDG assessment. Geneva. https://www.unicef.org/publications/index_82419.html. Accessed 27 July 2017

2. Boehler M, Zwickenpflug B, Hollender J et al (2012) Removal of micropollutants in municipal wastewater treatment plants by powder-activated carbon. Water Sci Technol 66:2115–2121

3. Rodriguez-Mozaz S, López De Alda MJ, Barceló D (2004) Monitoring of estrogens, pesticides and bisphenol A in natural waters and drinking water treatment plants by solid-phase extraction-liquid chromatography-mass spectrometry. J Chromatogr A 1045: 85–92. doi:10.1016/j.chroma.2004.06.040

4. Menon VC, Komarneni S (1998) Porous adsorbents for vehicular natural gas storage: a review. J Porous Mater 5:43–58. doi:10.1023/A:1009673830619

5. Alabadi A, Razzaque S, Yang Y et al (2015) Highly porous activated carbon materials from carbonized biomass with high CO_2 capturing capacity. Chem Eng J 281:606–612. doi:10.1016/j.cej.2015.06.032

6. Wei H, Deng S, Hu B et al (2012) Granular bamboo-derived activated carbon for high CO_2 adsorption: the dominant role of narrow micropores. ChemSusChem 5:2354–2360. doi:10.1002/cssc.201200570

7. Lo SF, Wang SY, Tsai MJ, Lin LD (2012) Adsorption capacity and removal efficiency of heavy metal ions by Moso and Ma bamboo activated carbons. Chem Eng Res Des 90:1397–1406. doi:10.1016/j.cherd.2011.11.020

8. Wang SY, Tsai MH, Lo SF, Tsai MJ (2008) Effects of manufacturing conditions on the adsorption capacity of heavy metal ions by Makino bamboo charcoal. Bioresour Technol 99:7027–7033. doi:10.1016/j.biortech.2008.01.014

9. Choy KKH, Barford JP, McKay G (2005) Production of activated carbon from bamboo scaffolding waste—process design, evaluation and sensitivity analysis. Chem Eng J 109:147–165. doi:10.1016/j.cej.2005.02.030

10. Lakkad SC, Patel JM (1981) Mechanical properties of bamboo, a natural composite. Fibre Sci Technol 14:319–322. doi:10.1016/0015-0568(81)90023-3

11. Chung KF, Yu WK (2002) Mechanical properties of structural bamboo for bamboo scaffoldings. Eng Struct 24:429–442. doi:10.1016/S0141-0296(01)00110-9

12. Bonilla SH, Guarnetti RL, Almeida CMVB, Giannetti BF (2010) Sustainability assessment of a giant bamboo plantation in Brazil: exploring the influence of labour, time and space. J Clean Prod 18: 83–91. doi:10.1016/j.jclepro.2009.07.012

13. Singh AN, Singh JS (1999) Biomass, net primary production and impact of bamboo plantation on soil redevelopment in a dry tropical region. For Ecol Manag 119:195–207. doi:10.1016/S0378-1127(98)00523-4

14. Kleinhenz V, Midmore DJ (2001) Aspects of bamboo agronomy. Adv Agron 74:99–145. doi:10.1016/S0065-2113(01)74032-1

15. Scurlock JMO, Dayton DC, Hames B (2000) Bamboo: an overlooked biomass resource? Biomass Bioenergy 19:229–244. doi:10.1016/S0961-9534(00)00038-6

16. Yamashita Y, Shono M, Sasaki C, Nakamura Y (2010) Alkaline peroxide pretreatment for efficient enzymatic saccharification of bamboo. Carbohydr Polym 79:914–920. doi:10.1016/j.carbpol.2009.10.017

17. Anca-Couce A (2016) Reaction mechanisms and multi-scale modelling of lignocellulosic biomass pyrolysis. Prog Energy Combust Sci 53:41–79. doi:10.1016/j.pecs.2015.10.002

18. Di Blasi C (1996) Kinetic and heat transfer control in the slow and flash pyrolysis of solids. Ind Eng Chem Res 35:37–46. doi:10.1021/ie950243d

19. Rodriguez Correa C, Otto T, Kruse A (2017) Influence of the biomass components on the pore formation of activated carbon. Biomass Bioenergy 97:53–64. doi:10.1016/j.biombioe.2016.12.017

20. George A, Morgan TJ, Kandiyoti R (2014) Pyrolytic reactions of lignin within naturally occurring plant matrices: challenges in biomass pyrolysis modeling due to synergistic effects. Energy Fuel 28:6918–6927. doi:10.1021/ef501459c

21. Forchheim D, Hornung U, Kruse A, Sutter T (2014) Kinetic modelling of hydrothermal lignin depolymerisation. Waste Biomass Valoriz 5:985–994. doi:10.1007/s12649-014-9307-6

22. Dinjus E, Kruse A, Tröger N (2011) Hydrothermal carbonization—1. Influence of lignin in lignocelluloses. Chem Eng Technol 34: 2037–2043. doi:10.1002/ceat.201100487

23. Ahmadpour A, Do DD (1996) The preparation of active carbons from coal by chemical and physical activation. Carbon N Y 34: 471–479. doi:10.1016/0008-6223(95)00204-9

24. Ahmadpour A, Do DD (1997) The preparation of activated carbon from macadamia nutshell by chemical activation. Carbon N Y 35: 1723–1732. doi:10.1016/S0008-6223(97)00127-9

25. Lillo-Ródenas M, Lozano-Castelló D, Cazorla-Amorós D, Linares-Solano A (2001) Preparation of activated carbons from Spanish anthracite: II. Activation by NaOH. Carbon N Y 39:751–759. doi:10.1016/S0008-6223(00)00186-X

26. Lozano-Castelló D, Lillo-Ródenas MA, Cazorla-Amorós D, Linares-Solano A (2001) Preparation of activated carbons from Spanish anthracite—I. Activation by KOH. Carbon N Y 39:741–749. doi:10.1016/S0008-6223(00)00185-8

27. Deutsches Institut für Normung e.V (2014) DIN 51732:2007-08 - Prüfung fester Brennstoffe - Bestimmung des Gesamtgehaltes an Kohlenstoff, Wasserstoff und Stickstoff - Instrumentelle Methoden

28. Deutsches Institut für Normung e.V (2010) DIN EN 14775:2010-04 Feste Biobrennstoffe – Bestimmung des Aschegehaltes

29. Deutsches Institut für Normung e.V (1997) DIN 51719:1997-07 - Pürfung fester Brennstoffe - Bestimmung des Aschegehaltes

30. Deutsches Institut für Normung e.V (2005) DIN EN 12904:2005-06 - Produkte zur Aufbereitung von Wasser für den menschlichen Gebrauch – Quarzsand und Quarzkies

31. ASTM International (2012) ASTM D7582 - Standard Test Methods for Proximate Analysis of Coal and Coke by Macro Thermogravimetric Analysis. doi:10.1520/D7582

32. Deutsches Institut für Normung e.V (2001) DIN 51720:2001-03 - Prüfung fester Brennstoffe - Bestimmung des Gehaltes an Flüchtigen Bestandteilen

33. Deutsches Institut für Normung e.V (2008) DIN 51734:2008-12 - Prüfung fester Brennstoffe - Immediatanalyse und Berechnung des Fixen Kohlenstoffs

34. Deutsches Institut für Normung e.V (2010) DIN ISO 9277:2014-01 - Determination of the specific surface area of solids by gas adsorption - BET method

35. Rouquerol J, Rouquerol F, Llewellyn P, et al (2013) Adsorption by powders and porous solids: principles, methodology and applications. Acad Press, London

36. Rodriguez Correa C, Bernardo M, Ribeiro RPPL et al (2017) Evaluation of hydrothermal carbonization as a preliminary step for the production of functional materials from biogas digestate. J Anal Appl Pyrolysis 124:461–474. doi:10.1016/j.jaap.2017.02.014

37. Dieguez-Alonso A, Anca-Couce A, Zobel N, Behrendt F (2015) Understanding the primary and secondary slow pyrolysis mechanisms of holocellulose, lignin and wood with laser-induced fluorescence. Fuel 153:102–109. doi:10.1016/j.fuel.2015.02.097

38. Sevilla M, Fuertes AB (2009) Chemical and structural properties of carbonaceous products obtained by hydrothermal carbonization of saccharides. Chem A Eur J 15:4195–4203. doi:10.1002/chem.200802097

39. Funke A, Reebs F, Kruse A (2013) Experimental comparison of hydrothermal and vapothermal carbonization. Fuel Process Technol 115:261–269. doi:10.1016/j.fuproc.2013.04.020

40. Reza MT, Lynam JG, Uddin MH, Coronella CJ (2013) Hydrothermal carbonization: fate of inorganics. Biomass Bioenergy 49:86–94. doi:10.1016/j.biombioe.2012.12.004

41. Chandra TC, Mirna MM, Sunarso J et al (2009) Activated carbon from durian shell: preparation and characterization. J Taiwan Inst Chem Eng 40:457–462. doi:10.1016/j.jtice.2008.10.002

42. Muniandy L, Adam F, Mohamed AR, Ng E-P (2014) The synthesis and characterization of high purity mixed microporous/mesoporous activated carbon from rice husk using chemical activation with NaOH and KOH. Microporous Mesoporous Mater 197:316–323. doi:10.1016/j.micromeso.2014.06.020

43. Nowakowski D, Jones J, Brydson R, Ross A (2007) Potassium catalysis in the pyrolysis behaviour of short rotation willow coppice. Fuel 86:2389–2402. doi:10.1016/j.fuel.2007.01.026

44. Ross RA, Fong P (1981) The conversion of cellulose to fuel gases promoted by selected solid additives. Conserv Recycl 4:15–28. doi:10.1016/0361-3658(81)90004-7

45. Nowakowski DJ, Woodbridge CR, Jones JM (2008) Phosphorus catalysis in the pyrolysis behaviour of biomass. J Anal Appl Pyrolysis 83:197–204. doi:10.1016/j.jaap.2008.08.003

46. Di Blasi C, Branca C, D'Errico G (2000) Degradation characteristics of straw and washed straw. Thermochim Acta 364:133–142. doi:10.1016/S0040-6031(00)00634-1

47. McKee DW (1983) Mechanisms of the alkali metal catalysed gasification of carbon. Fuel 62:170–175. doi:10.1016/0016-2361(83)90192-8

48. Marsh H, Rodríguez-Reinoso F (2006) Activated carbon. Act Carbon. doi:10.1016/B978-008044463-5/50019-4

49. Sevilla M, Fuertes AB, Mokaya R (2011) High density hydrogen storage in superactivated carbons from hydrothermally carbonized renewable organic materials. Energy Environ Sci 4:1400. doi:10.1039/c0ee00347f

50. Sun Y, Gao B, Yao Y et al (2014) Effects of feedstock type, production method, and pyrolysis temperature on biochar and hydrochar properties. Chem Eng J 240:574–578. doi:10.1016/j.cej.2013.10.081

51. Kim KH, Kim JY, Cho TS, Choi JW (2012) Influence of pyrolysis temperature on physicochemical properties of biochar obtained from the fast pyrolysis of pitch pine (Pinus rigida). Bioresour Technol 118:158–162. doi:10.1016/j.biortech.2012.04.094

52. Illán-Gómez MJ, García-García A, Salinas-Martínez de Lecea C, Linares-Solano A (1996) Activated carbons from Spanish coals. 2. Chemical activation. Energy Fuel 10:1108–1114. doi:10.1021/ef950195+

53. Hirunpraditkoon S, Tunthong N, Ruangchai A, Nuithitikul K (2011) Adsorption capacities of activated carbons prepared from bamboo by KOH activation. Int J Chem Mol Nucl Mater Metall Eng 5:477–481

54. Basta AH, Fierro V, El-Saied H, Celzard A (2009) 2-Steps KOH activation of rice straw: an efficient method for preparing high-performance activated carbons. Bioresour Technol 100:3941–3947. doi:10.1016/j.biortech.2009.02.028

55. Lillo-Ródenas MA, Marco-Lozar JP, Cazorla-Amorós D, Linares-Solano A (2007) Activated carbons prepared by pyrolysis of mixtures of carbon precursor/alkaline hydroxide. J Anal Appl Pyrolysis 80:166–174. doi:10.1016/j.jaap.2007.01.014

56. Hill A, Marsh H (1968) A study of the adsorption of iodine and acetic acid from aqueous solutions on characterized porous carbons. Carbon N Y 6:31–39. doi:10.1016/0008-6223(68)90048-1

57. Graham D (1955) Characterization of physical adsorption systems. III The separate effects of pore size and surface acidity upon the adsorbent capacities of activated carbons. J Phys Chem 59:896–900. doi:10.1021/j150531a022

58. Singh B, Madhusudhanan S, Dubey V et al (1996) Active carbon for removal of toxic chemicals from contaminated water. Carbon N Y 34:327–330. doi:10.1016/0008-6223(95)00179-4

59. Wu F-C, Tseng R-L, Juang R-S (1999) Preparation of activated carbons from bamboo and their adsorption abilities for dyes and phenol. J Environ Sci Heal Part A 34:1753–1775. doi:10.1080/10934529909376927

60. Kim BC, Kim YH, Yamamoto T (2008) Adsorption characteristics of bamboo activated carbon. Korean J Chem Eng 25:1140–1144. doi:10.1007/s11814-008-0187-y

61. Niaz S, Manzoor T, Pandith AH (2015) Hydrogen storage: materials, methods and perspectives. Renew Sust Energ Rev 50:457–469. doi:10.1016/j.rser.2015.05.011

62. Georgakis M, Stavropoulos G, Sakellaropoulos GP (2007) Molecular dynamics study of hydrogen adsorption in carbonaceous microporous materials and the effect of oxygen functional groups. Int J Hydrog Energy 32:1999–2004. doi:10.1016/j.ijhydene.2006.08.040

63. Thomas KM (2009) Adsorption and desorption of hydrogen on metal–organic framework materials for storage applications: comparison with other nanoporous materials. Dalton Trans 0:1487. doi:10.1039/b815583f

64. Lozano-Castelló D, Suárez-García F, Linares-Solano Á, Cazorla-Amorós D (2013) Chapter 12 - Advances in hydrogen storage in carbon materials. In: Renew. Hydrog. Technol. Elsevier, Amsterdam, pp 269–291

65. Broom DP (2011) Hydrogen storage materials. Springer, London

66. Lozano-Castelló D, Cazorla-Amorós D, Linares-Solano A, Quinn DF (2002) Activated carbon monoliths for methane storage: influence of binder. Carbon N Y 40:2817–2825. doi:10.1016/S0008-6223(02)00194-X